OPEN ACCESS
IOP Publishing
Journal of Physics B: Atomic, Molecular and Optical Physics
J. Phys. B: At. Mol. Opt. Phys. **49** (2016) 134004 (9pp)
doi:10.1088/0953-4075/49/13/134004

The role of antihydrogen formation in the radial transport of antiprotons in positron plasmas

S Jonsell[1], M Charlton[2] and D P van der Werf[2,3]

[1] Department of Physics, Stockholm University, SE-10691, Stockholm, Sweden
[2] Department of Physics, College of Science, Swansea University, Swansea SA2 8PP, UK
[3] IRFU, CEA, Saclay, F-91191, Gif-sur-Yvette Cedex, France

E-mail: jonsell@fysik.su.se

Received 4 February 2016, revised 20 April 2016
Accepted for publication 4 May 2016
Published 1 June 2016

Abstract

Simulations have been performed of the radial transport of antiprotons in positron plasmas under ambient conditions typical of those used in antihydrogen formation experiments. The parameter range explored includes several positron densities and temperatures, as well as two different magnetic fields (1 and 3 T). Computations were also performed in which the antihydrogen formation process was artificially suppressed in order to isolate its role from other collisional sources of transport. The results show that, at the lowest positron plasma temperatures, repeated cycles of antihydrogen formation and destruction are the dominant source of radial (cross magnetic field) transport, and that the phenomenon is an example of anomalous diffusion.

Keywords: antihydrogen, antiprotons, transport, positron, plasma

(Some figures may appear in colour only in the online journal)

1. Introduction

Recent years have seen many advances in studies with antihydrogen, $\overline{\mathrm{H}}$. These have included: the first formation experiments involving the controlled mixing of antiprotons and positrons [1, 2]; the successful trapping of small samples of the anti-atoms in magnetic minimum neutral atom traps [3–6]; the demonstration of beam-like propagation of antihydrogen [7, 8] and the first explorations of its properties [9–12]. This work was undertaken at the unique Antiproton Decelerator facility located at CERN [13, 14] which supplies pulses of 5.3 MeV antiprotons ($\overline{p}$s) every 100 s or so for subsequent experimentation.

One of the basic instruments used for almost all antihydrogen experiments to date is the Penning, or Penning–Malmberg, trap. These are examples of charged particle traps (see e.g., [15–17]) which are used to collect, control and manipulate $\overline{p}$ and positron (e^+) clouds and plasmas, and to mix them to form the anti-atoms. Such traps employ strong magnetic fields (typically of tesla strength) for radial confinement of the charged species, as the field is directed along the axis of a series of electrodes, with the latter suitably electrically biased to provide the axial confinement. To date, almost all antihydrogen experiments have involved mixing antiprotons and positrons in a so-called nested Penning trap environment [18] in which typical e^+ cloud/plasma temperatures, T_e, have been below 100 K (though this parameter was not always directly measured) and with densities in the range from $n_e = 10^{13}$–10^{15} m^{-3}. It has been found that antihydrogen is typically formed via the three-body interaction given by

$$\overline{p} + e^+ + e^+ \rightarrow \overline{\mathrm{H}}^{**} + e^+. \quad (1)$$

It has been well-documented how the nascent anti-atoms are very weakly bound (by of the order of $k_B T_e$ for reaction (1) [19–21], where their excited nature is denoted by the double-star superscript), and are thus susceptible to influence from

the local fields, and in particular the trap electric field, and the e^+ plasma self-field. The influence of these has been observed in several experiments in which field ionisation of the anti-atoms has resulted in $\overline{p}$ separation from the e^+ plasma [22, 23], and has also been exploited as a means of probing antihydrogen formation and to gain insight into binding energies [2, 7, 8, 24].

The weakly bound newly formed antihydrogen atoms may also be affected by collisions in the e^+ plasma: indeed, it has been emphasised elsewhere, and in particular in [21], how the antihydrogen that is detected is a result of a detailed sequence of processes which involve repeated cycles of antihydrogen formation according to reaction (1), and break-up in collision as

$$e^+ + \overline{\mathrm{H}}^{**} \rightarrow \overline{p} + e^+ + e^+. \tag{2}$$

This process is likely to have a very large cross section, probably in excess of geometric ($\sim 10^{-12}$ m^{-2}), leading to collision frequencies for $n_\mathrm{e} = 10^{14}$ m^{-3} of around 10^7 s^{-1}, which is much faster than the inverse of the time taken for an antihydrogen atom to travel 1 mm (about 1 μs). This reaction will also be in competition with de-excitation of the $\overline{\mathrm{H}}^{**}$,

$$e^+ + \overline{\mathrm{H}}^{**} \rightarrow \overline{\mathrm{H}}^{*} + e^+, \tag{3}$$

which may lead to a state stable against subsequent ionisation. The overall equilibrium rate for the production of stable anti-atoms through three-body recombination (1) and subsequent collisional stabilisation (3) is proportional to $n_\mathrm{e}^2 T_\mathrm{e}^{-4.5}$ (see e.g., [19, 25, 26] for further discussion). (Note that radiative recombination is an alternative route to $\overline{\mathrm{H}}$ formation and is expected to preferentially produce low-lying, deeply bound states at low rate: see e.g., [25]. This process will deplete the $\overline{p}$ cloud, but will not otherwise disturb it, nor the positron plasma, and it is therefore not included in the discussion here.)

Following the initial ATHENA and ATRAP experiments [1, 2, 22, 24, 27–30] a number of authors undertook simulations and theoretical analyses of various aspects of antihydrogen formation, as applied to the experimental situations [31–41], and as summarised by Robicheaux [20].

In this spirit, a detailed examination of antihydrogen formation was undertaken by Jonsell *et al* [21] under simulated conditions appropriate to those of the ATHENA experiment, and the present work is in part based upon some of their observations. They found that the fraction of time that an antiproton spends bound as antihydrogen is usually small, typically less than 1% (at $T_\mathrm{e} = 15$ K and n_e up to 10^{15} m^{-3}). This was interpreted as being due to the rate of the two-body destruction process, reaction (2), greatly exceeding that for the three-body formation rate of reaction (1), due to, as mentioned above, the very large cross section for break-up. Furthermore, they found that the radial distributions of the antiprotons were time-dependent. This was attributed to cross-magnetic field drift of the $\overline{p}$s while neutralised as antihydrogen, before break-up, but with the latter occurring at a larger (on average) radius, r (with $r = 0$ the z- and B-field axis of the system) than the formation event.

Thus, as time proceeds during a e^+–$\overline{p}$ mixing experiment, the antiprotons progressively move towards the outer edge of the positron plasma. The importance of this is that here the combination of the plasma self electric field $\mathbf{E} = n_\mathrm{e} e\mathbf{r}/2\epsilon_0 = E\hat{\mathbf{r}}$ (which is radial, $\mathbf{r} = r\hat{\mathbf{r}}$, in nature with e the elementary charge and ϵ_0 the permittivity of free space) and the uniform axial magnetic field, $\mathbf{B} = B\hat{\mathbf{z}}$, provided in the experiment by a solenoid results in an antiproton tangential speed given by $v_\mathrm{T} = E/B = n_\mathrm{e} e r/2\epsilon_0 B$, proportional to the radial position of the $\overline{p}$. As an example, take $r = 1$ mm, $B = 1$ T and $n_\mathrm{e} = 10^{14}$ m^{-3}, to find $v_\mathrm{T} \sim 900$ ms^{-1}, which corresponds to an effective temperature/equivalent kinetic energy of around 33 K. This is to be compared to typical antihydrogen trap depths, which are around 0.5 K. Thus, it is clear that if antihydrogen is formed in dense positron plasmas the radial position of creation will have a direct bearing on the ability to trap the anti-atom for further study.

Motivated by the results of the earlier simulations [21], and the importance to the aforementioned experiments involving antihydrogen trapping and also to the creation of beams of (ground state) anti-atoms for hyperfine spectroscopy, we have performed a more detailed study of $\overline{p}$ radial transport in dense, cold e^+ plasmas during antihydrogen formation. We have explored the positron density range from 10^{13}–10^{15} m^{-3}, with positron temperatures between 10 and 50 K, and for applied magnetic fields of 1 and 3 T. The higher n_e and B are typical of early experiments (e.g,. ATHENA [1, 22, 30]) for which there are data to which semi-quantitative comparisons can be made. More recently lower B fields have been used to help promote $\overline{\mathrm{H}}$ capture in magnetic minimum traps, typically alongside lower n_e which has been found to be helpful in the quest for lower $\overline{\mathrm{H}}$ temperatures.

The methodology we have adopted is described in section 2, with our results and discussion presented in section 3. We draw our conclusions in section 4.

2. Simulation methodology

The simulations were performed using the methodology developed, and described fully, by Jonsell *et al* [21]: thus, we need only provide a brief summary here. The $\overline{p}$ trajectories were computed using classical equations of motion, along with those of any e^+s within a cylinder of radius and height $n_\mathrm{e}^{-1/3}$. The use of classical equations is valid since quantum mechanical effects are only relevant on much smaller length scales than those of the typical e^+–$\overline{p}$ interactions under the plasma conditions considered here. The particle trajectories were found by integrating Newton's equations of motion for the Lorentz force $\mathbf{F} = \pm e(\mathbf{E} + \mathbf{v} \times \mathbf{B})$, where, as above, $\mathbf{B}$ is a uniform solenoid field (i.e., we do not attempt to model the situation in which an additional non-uniform magnetic field is applied to confine some of the anti-atoms, though this will typically be a minor perturbation due to the small plasma size relative to the atom trap). In this work we focus on the motion of antiprotons *inside* the positron plasma, where the electric field is the plasma self electric field ($\mathbf{E}$, as defined

above) and has no axial component. The number of trajectories was usually 20 000 for each parameter setting.

Since this study does not seek to simulate experimental procedures, which typically involve various means of injecting the antiprotons into the positron plasma, the antiproton trajectories were initialised at zero radius, with a thermal velocity distribution (set by T_e) in the radial and axial directions. Our simulation distinguishes free antiprotons from those bound inside an antihydrogen atom. In the former case the charged particle is subject to a drag force from the plasma [42], as well as a diffusive force related to the drag by the fluctuation dissipation theorem. While bound as a neutral antihydrogen atom the antiproton is not subject to these forces, and instead the interaction with the one or more positrons present is calculated explicitly. This procedure necessitates a clear distinction between bound states and continuum states of any positrons in the vicinity of the antiproton. In the presence of strong magnetic and electric fields typical of antihydrogen experiments, this separation is not well defined. Thus, in our simulations we calculate large numbers of many-positron antiproton collisions and any collision ending with a positron bound to an antiproton by more than $k_B T_e$ (the binding energy calculated without including external electric and magnetic fields) is defined as formation of an antihydrogen atom. The rate of such events is evaluated (see table 2), and the positron state after the collision is saved as the initial condition for an antihydrogen atom.

Our main observable is the radial position of the antiproton, as a function of time. We can also track other quantities such as the change in radial position, Δr, of each jump, the binding energy of the antihydrogen formed etc. We can vary external conditions such as plasma temperature, density (and hence electric field) and magnetic field.

3. Results and discussion

Though our simulations assume that the positrons and antiprotons are in thermal equilibrium, the nature of the $\overline{\mathrm{H}}$ formation and break-up cycles (reactions (1) and (2)) mean that the rate of stable (against break-up, say via reaction (3), and which might thus be observed by experiment) $\overline{\mathrm{H}}$ production and the transient rate of $\overline{\mathrm{H}}$ formation in the positron plasma, are not the same. It is expected that the latter will be much higher than the former, and they will not necessarily have the same dependence upon T_e. In the analysis presented after the discussion of the simulation results, we attempt to estimate the overall rates of $\overline{\mathrm{H}}$ production and break-up in the positron plasma, as it is these that, under circumstances elucidated by the present study, can govern the cross-field transport of the antiprotons.

When a neutral antihydrogen atom is formed its centre-of-mass motion will cease to be influenced by the electric and magnetic fields in the plasma, though its momentum vector will be dominated by that of the antiproton at the moment of antihydrogen formation. The antihydrogen will continue largely in the same direction until it is again ionised, and the $\overline{p}$ resumes its circular motion around the axis of the trap. It will, however, now circulate at a different trap radius because of the motion it made while bound as antihydrogen. Thus, an antiproton will make a radial 'jump' $\Delta r_{\overline{\mathrm{H}}}$ every time it is bound transiently as an antihydrogen atom.

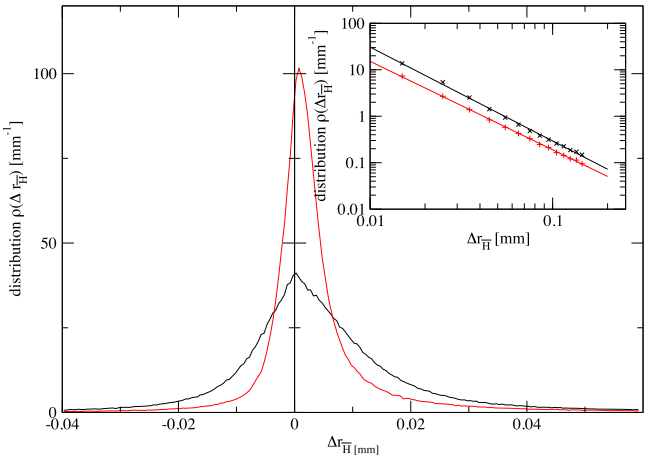

Figure 1. Distribution of changes in radial position $\Delta r_{\overline{\mathrm{H}}}$ of an antiproton between the times of formation and ionisation of an antihydrogen atom. Temperature $T_e = 15$ K, density $n_e = 10^{15}$ m^{-3}, and magnetic fields $B = 1$ T (black) and 3 T (red). The inset shows the large $r_{\overline{\mathrm{H}}}$ tails on a log–log scale, including fits to a distribution $\propto(\Delta r_{\overline{\mathrm{H}}})^n$, where $n = 2.0$ for $B = 1$ T and $n = 1.9$ for 3 T.

The size of these 'jumps' will follow some distribution $\rho(\Delta r_{\overline{\mathrm{H}}})$. Examples of our simulated results for such distributions are shown in figure 1. If the motion of the $\overline{p}$s were only due to thermal effects, one would expect a $\Delta r_{\overline{\mathrm{H}}}$ distribution symmetric around $\Delta r_{\overline{\mathrm{H}}} = 0$. In contrast, if the radial drift were only due to the tangential velocity component arising from the $\mathbf{E} \times \mathbf{B}$ drift motion one would always have $\Delta r_{\overline{\mathrm{H}}} > 0$. Hence, the combination of these two effects gives a distribution with both negative and positive $\Delta r_{\overline{\mathrm{H}}}$, but with a bias towards positive jumps. This will be discussed in more detail below.

Considering radial motion due to antihydrogen formation only, starting from $r = 0$, the radial position at some later time, t_N, will be the sum of all N jumps, $r(t_N) = \sum_{i=1}^{N}(\Delta r_{\overline{\mathrm{H}}})_i$. The time required to make N jumps is on average given by N divided by the antihydrogen formation rate $\lambda_{\overline{\mathrm{H}}}$ increased by the time the $\overline{p}$ spends as an $\overline{\mathrm{H}}$, $t_N = N/\lambda_{\overline{\mathrm{H}}} + \sum_{i=1}^{N}(\Delta t)_i$. Hence, the average radial $\overline{p}$ speed due to antihydrogen formation is given by

$$\langle v_{\overline{\mathrm{H}}}\rangle \simeq \frac{\sum_{i=1}^{N}(\Delta r_{\overline{\mathrm{H}}})_i}{N/\lambda_{\overline{\mathrm{H}}} + \sum_{i=1}^{N}(\Delta t)_i} = \frac{\lambda_{\overline{\mathrm{H}}}\frac{1}{N}\sum_{i=1}^{N}(\Delta r_{\overline{\mathrm{H}}})_i}{1 + \lambda_{\overline{\mathrm{H}}}\frac{1}{N}\sum_{i=1}^{N}(\Delta t)_i} = (1 - F_{\overline{\mathrm{H}}})\lambda_{\overline{\mathrm{H}}}\langle\Delta r_{\overline{\mathrm{H}}}\rangle, \quad (4)$$

where $F_{\overline{\mathrm{H}}} = \langle\Delta t\rangle/(1/\lambda_{\overline{\mathrm{H}}} + \langle\Delta t\rangle)$ (with $\langle\Delta t\rangle = \frac{1}{N}\sum_{i=1}^{N}(\Delta t)_i$) is the fraction of time the $\overline{p}$ spends as $\overline{\mathrm{H}}$. The average $\Delta r_{\overline{\mathrm{H}}}$ can also be written as

$$\langle\Delta r_{\overline{\mathrm{H}}}\rangle = \int_{-r_0}^{\infty} r\rho(r)\mathrm{d}r, \quad (5)$$

where r_0 is the radial position before the jump.

Table 1. Exponents of large $\Delta r_{\overline{\mathrm{H}}}$ jump size distributions $\propto(\Delta r_{\overline{\mathrm{H}}})^n$.

T_e (K)	n_e (m^{-3})	B (T)	n
15	10^{15}	1	2.0
15	10^{15}	3	1.9
30	10^{15}	1	1.7
30	10^{15}	3	1.7
15	5×10^{14}	1	1.6
15	10^{14}	1	0.9
15	5×10^{13}	1	1.0

It is therefore interesting to study how the distribution $\rho(\Delta r_{\overline{\mathrm{H}}})$ falls off for long $\Delta r_{\overline{\mathrm{H}}}$ (see the inset of figure 1). The large $\Delta r_{\overline{\mathrm{H}}}$ tail of the distribution will, through the influence of Δt, have a very complicated dependence on the binding energies of the $\overline{\mathrm{H}}$s formed, and how the binding energy evolves as the $\overline{\mathrm{H}}$ undergoes further collisions. We find this behaviour by fitting to simulated data, such that the tail is well described by a power law $(\Delta r_{\overline{\mathrm{H}}})^{-n}$, with $1 \lesssim n \lesssim 2$ for different parameters (see table 1). Our data indicate that the distribution falls off more slowly at small densities, which can be expected, as at higher densities the collision frequency is higher, and thus Δt shorter. In fact, due to the slow fall off the integral in (5) diverges, as is characteristic for anomalous diffusion influenced by Lévy flights [43]. This necessitates a cut-off in the $\Delta r_{\overline{\mathrm{H}}}$ distribution, which we will discuss further.

In addition to the change in radial position when neutral as $\overline{\mathrm{H}}$, there is also, as explained in section 2, diffusive drift of the bare $\overline{p}$s. Considering this drift alone, we can write the diffusion as a series of small jumps in the x- and y-directions: $(x_N, y_N) = \left(\sum_{i=1}^{N}\Delta x_i, \sum_{i=1}^{N}\Delta y_i\right)$ with zero average $\langle(x_N, y_N)\rangle = (0, 0)$. Note, that these displacements are relative the bulk motion of the plasma, i.e. take place in a reference frame rotating with the $\mathbf{E} \times \mathbf{B}$ drift velocity of the positron plasma. Looking at the mean square radial displacement

$$\langle r_N^2\rangle = \langle x_N^2\rangle + \langle y_N^2\rangle = \left\langle \sum_{i=1}^{N}\Delta x_i \sum_{j=1}^{N}\Delta x_j \right\rangle + \left\langle \sum_{i=1}^{N}\Delta y_i \sum_{j=1}^{N}\Delta y_j \right\rangle = \left\langle \sum_{i=1}^{N}(\Delta x_i)^2 \right\rangle + \left\langle \sum_{i=1}^{N}(\Delta y_i)^2 \right\rangle = N\Delta r_{\overline{p}}^2, \tag{6}$$

where the average of $(\Delta x_i)^2$ and $(\Delta y_i)^2$ is $\Delta r_{\overline{p}}^2/2$. Since we here consider only the thermal drift, which is made up of much more frequent and smaller jumps (as compared to the radial jumps induced by antihydrogen formation), we consider this as a continuous process, relating the number of jumps to time t, through $N = \lambda_{\mathrm{ep}}t$, where λ_{ep} is the positron–antiproton collision frequency. We can also define the usual diffusion coefficient D through $\langle(r(t) - r(0))^2\rangle = \lambda_{\mathrm{ep}}\Delta r_{\overline{p}}^2 t = 2Dt$. We will return to this below.

The magnetic field dependence of the collision frequency, as well as of the jump size distribution, is not dramatic, leading to a similar rate of radial transport for different field strengths. The antihydrogen formation rate is, however, reduced by a factor of around 20 when the temperature is doubled from 15 to 30 K: see table 2. This, coupled to a not too different jump-size distribution, gives a dramatically reduced rate of radial transport as the temperature is increased. In fact, at higher temperatures normal thermal drift dominates.

Table 2. The frequency, $\lambda_{\overline{\mathrm{H}}}$, of antihydrogen formation events in the plasma. A formation event is defined as a three-body collision which results in a $\bar{p}e^+$ state with binding energy (calculated without including the external fields) larger than $k_B T_e$, where T_e is the plasma temperature.

T_e (K)	n_e (m^{-3})	B (T)	$\lambda_{\overline{\mathrm{H}}}$ (s^{-1})
15	10^{15}	1	9.7×10^4
30	10^{15}	1	5.0×10^3
10	10^{15}	3	4.8×10^5
15	10^{15}	3	8.2×10^4
20	10^{15}	3	2.4×10^4
25	10^{15}	3	9.2×10^3
30	10^{15}	3	4.2×10^3
50	10^{15}	3	4.8×10^2

The slow fall off for large $\Delta r_{\overline{\mathrm{H}}}$ in figure 1 makes the radial position of the antiprotons, when averaged over many trajectories, very sensitive to a small number of trajectories involving very large radial jumps. This makes the average difficult to calculate, or even undefined. We therefore need to introduce a cut-off radius $r_c = 1$ mm, removing any antiprotons which cross this radius from the average. This is physically motivated by the finite radius of any real positron plasma (assuming that the antihydrogen is field-ionised outside the plasma, or that any remaining radial transport outside the plasma is not interesting for our purposes). As a consequence, when radial transport is significant, the average will approach, but never cross r_c. At the same time the average will be taken over a decreasing number of trajectories (since some are removed because they crossed the cut-off radius), leading to increasing statistical fluctuations. This cut-off changes the upper limit of the integral in (5) to $r_c - r_0$ making the average $\langle\Delta r_{\overline{\mathrm{H}}}\rangle$ and the attendant speed $v_{\overline{\mathrm{H}}}$ well defined.

An example of the time evolution of the radial distribution of antiprotons is shown in figure 2. It can be seen that at short times most antiprotons are located well within the plasma (i.e. at $r < r_c = 1$ mm). As time progresses the peak of the distribution grows outwards. The distribution is sharply cut off at $r = r_c$, representing the outer radius of the positron plasma. The tail extending beyond r_c is removed from the simulation, with the effect that the integral of the distribution with time diminishes from its initial value 1.0, until in the end all antiprotons would have left the plasma (at 0.2 ms the integral is 0.7, while at 1.0 ms it is 0.12).

The results of our simulations for various densities, temperatures and magnetic fields are shown in figure 3, and can be contrasted with those shown in figure 4, where antihydrogen formation was artificially turned off. The radial drift is then exclusively due to thermal Brownian motion, which is confirmed by good fits to $\langle(r(t) - r(0))^2\rangle \propto t$, when thermal diffusion is slow (we attribute the deviation from the linear dependence when the diffusion is fast to the velocity-

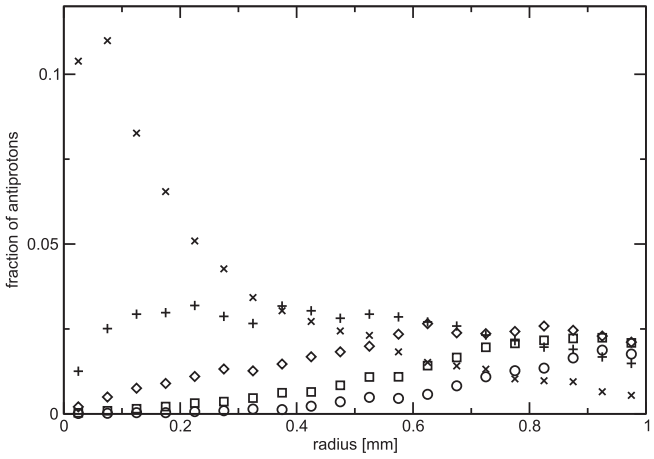

Figure 2. Time evolution of the average radial position of the antiprotons for $n_e = 10^{15}$ m^{-3}, $B = 3$ T and $T_e = 15$ K. The symbols represent different times, 0.2 ms (×), 0.4 ms (+), 0.6 ms (◇), 0.8 ms (□), and 1.0 ms (○). In the simulation 20000 antiprotons were initiated at $r = 0$. Note that the distribution is cut off at $r_c = 1$ mm (see text).

dependence of the friction coefficients from [42], and the difference at large positron densities between the drift velocity of the e^+s and the $\bar{p}$s [21]). Here, the effect of the magnetic field is more important than the temperature, since it pins the charged particles to field lines, thus inhibiting radial motion.

The temperature dependence of the radial drift is examined in figure 5. As expected the radial drift is much slower at higher temperatures. We find that the drift varies sharply with the temperature of the positrons; at 10 K all simulated trajectories have crossed r_c within 1 ms. Increasing the temperature by only 5 K there are still antiprotons remaining up to 2 ms, but a significant fraction have left the plasma, as is visible by the trend towards saturation at r_c. At 50 K more than 90% of the antiprotons remain after 2 ms, but a small fraction has jumped by large Δr and either left the plasma or contributed to raising the average $(r(t) - r(0))^2$ significantly compared to thermal-only diffusion.

An experimentally relevant measure of the rate of radial antiproton drift is the fraction of antiprotons reaching the outer radius of the plasma, within a certain time. We plot this fraction after 2 ms as a function of density and magnetic field for a 15 K plasma in figure 6(a), which shows that it rises rapidly above about $n_e = 10^{14}$ m^{-3} due to the influence of $\overline{\mathrm{H}}$ formation by reaction (1). Again, the dependence on magnetic field is weak. In a 30 K plasma the time scale for the antiprotons to reach r_c is longer. For this temperature, and in the density range investigated, we have to wait between 0.01–0.1 s, to find a significant fraction of antiprotons at this radius, as can be seen in figure 6(b). At 15 K the antiproton radial drift contributes little, confirming that a mechanism involving the formation of antihydrogen is the dominant reason for radial transport.

In what follows, an attempt is made to develop a simple model of the transport of antiprotons in positron plasmas in an effort to underpin the results of the simulations. Combining the ballistic diffusion with speed $\langle v_{\overline{\mathrm{H}}} \rangle$ from (4), with the normal diffusion during the time $(1 - F_{\overline{\mathrm{H}}})t$ the $\overline{p}$ is free, we find

$$\langle (r(t) - r(0))^2 \rangle = (1 - F_{\overline{\mathrm{H}}})^2 \lambda_{\overline{\mathrm{H}}}^2 \langle \Delta r_{\overline{\mathrm{H}}}^2 \rangle t^2 + (1 - F_{\overline{\mathrm{H}}}) \lambda_{\mathrm{ep}} \langle \Delta r_{\overline{p}}^2 \rangle t, \tag{7}$$

where λ_{ep} is the positron–antiproton collision frequency and in which we have assumed that $\langle \Delta r_{\overline{\mathrm{H}}}^2 \rangle = \langle \Delta r_{\overline{\mathrm{H}}} \rangle^2$: see below. The average time required for the $\overline{p}$ to diffuse out to some radius r is then

$$t = \sqrt{\left[\frac{\lambda_{\mathrm{ep}} \langle \Delta r_{\overline{p}}^2 \rangle}{2(1 - F_{\overline{\mathrm{H}}}) \lambda_{\overline{\mathrm{H}}}^2 \langle \Delta r_{\overline{\mathrm{H}}}^2 \rangle} \right]^2 + \frac{r^2}{(1 - F_{\overline{\mathrm{H}}})^2 \lambda_{\overline{\mathrm{H}}}^2 \langle \Delta r_{\overline{\mathrm{H}}}^2 \rangle}} - \frac{\lambda_{\mathrm{ep}} \langle \Delta r_{\overline{p}}^2 \rangle}{2(1 - F_{\overline{\mathrm{H}}}) \lambda_{\overline{\mathrm{H}}}^2 \langle \Delta r_{\overline{\mathrm{H}}}^2 \rangle}. \tag{8}$$

There are two limits, (i) when $r \lambda_{\overline{\mathrm{H}}} \sqrt{\langle \Delta r_{\overline{\mathrm{H}}}^2 \rangle} \gg \lambda_{\mathrm{ep}} \langle \Delta r_{\overline{p}}^2 \rangle$ ballistic diffusion dominates and $t \simeq r/((1 - F_{\overline{\mathrm{H}}}) \lambda_{\overline{\mathrm{H}}} \sqrt{\langle \Delta r_{\overline{\mathrm{H}}}^2 \rangle})$ and (ii) in the opposite limit thermal diffusion dominates and $t \simeq r^2 / [(1 - F_{\overline{\mathrm{H}}}) \lambda_{\mathrm{ep}} \langle \Delta r_{\overline{p}}^2 \rangle]$. The relative importance of the two effects can be parameterised by the ratio

$$R = \frac{r \lambda_{\overline{\mathrm{H}}} \sqrt{\langle \Delta r_{\overline{\mathrm{H}}}^2 \rangle}}{\lambda_{\mathrm{ep}} \langle \Delta r_{\overline{p}}^2 \rangle}. \tag{9}$$

We now estimate the size of the $\overline{p}$ radial step in a collision with a positron. Positrons in the plasma have a speed $v_e = \sqrt{2 k_B T_e / (\pi m)}$ (since positrons are pinned to magnetic field lines we use the average of the one-dimensional Maxwell-Boltzmann distribution). Using momentum conservation we expect that $M \Delta v_{\bar{p}} \sim 2 m v_e$. Further using $v_{\bar{p}} \sim \Omega_c r_{\bar{p}}$, with $\Omega_c = e B / M$ the cyclotron frequency of the antiprotons, we find that

$$\Delta r_{\bar{p}} \sim 2 \frac{m}{M} \frac{v_e}{\Omega_c} = \frac{2}{eB} \sqrt{\frac{2 k_B T_e m}{\pi}}. \tag{10}$$

It is now assumed that the positron–antiproton collision frequency is given by $\lambda_{\mathrm{ep}} = n_e b^2 v_e$, with n_e the positron density and $b = e^2 / 4 \pi \epsilon_0 k_B T_e$ is the classical distance of closest approach. Here collisional suppression effects due to the presence of the strong B-field have been ignored. It can then be shown that

$$\lambda_{\mathrm{ep}} = \frac{n_e}{T_e^{3/2}} \left(\frac{e^4}{8 \sqrt{2} \pi^{5/2} \epsilon_0^2 k_B^{3/2} m^{1/2}} \right) \equiv C \frac{n_e}{T_e^{3/2}}. \tag{11}$$

The rate of cross-field transport (as an antiproton, distinct from antihydrogen) is proportional to $\lambda_{\mathrm{ep}} \Delta r_{\bar{p}}^2$, which can be written from (10) and (11) as

$$\lambda_{\mathrm{ep}} \Delta r_{\bar{p}}^2 = C \frac{8 n_e}{\pi T_e^{1/2}} \frac{k_B m}{(eB)^2}. \tag{12}$$

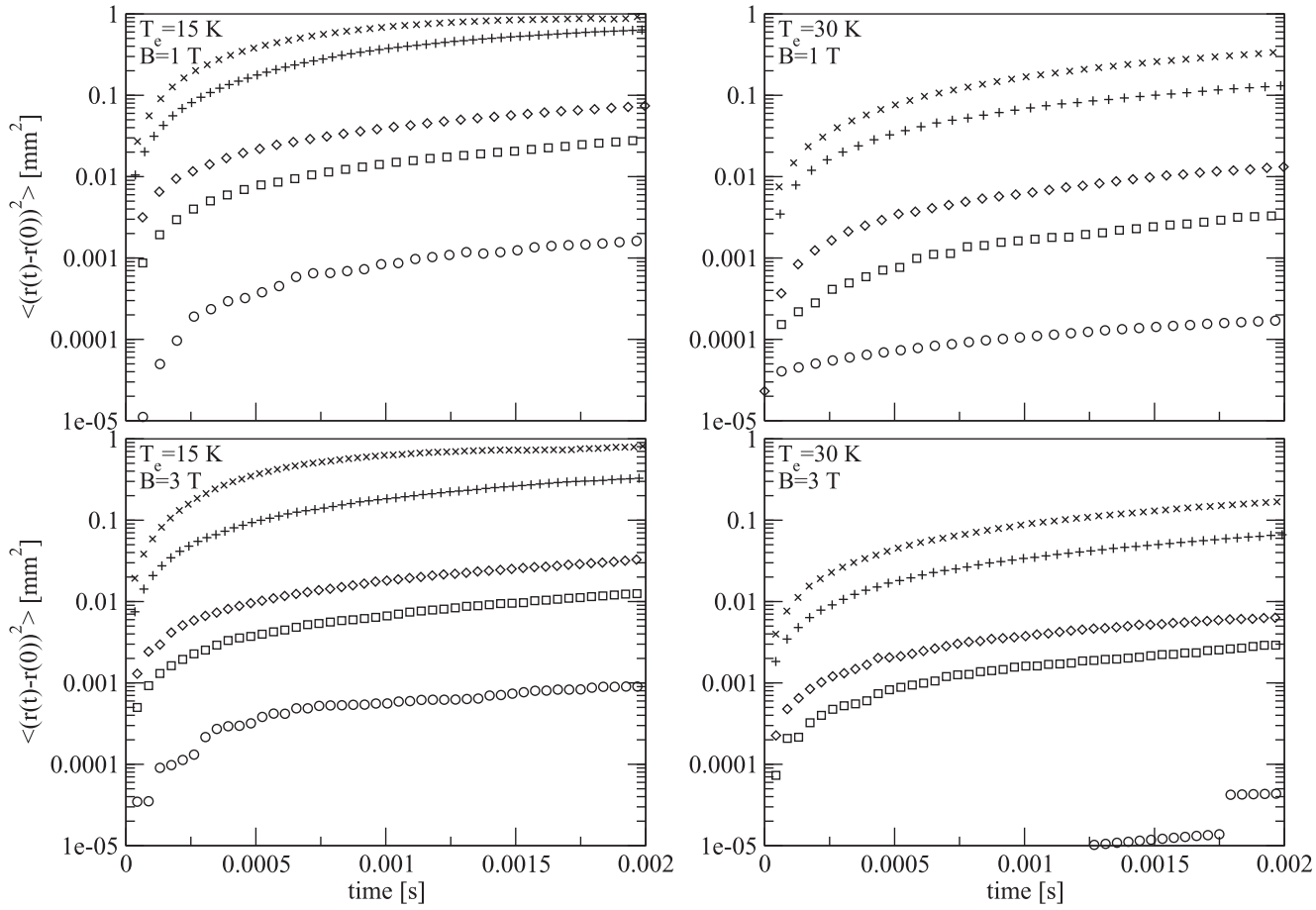

Figure 3. Time evolution of the average radial position of the antiproton, assuming a plasma radius of $r_c = 1$ mm. The values for the plasma temperature T_e and the magnetic field B are indicated in each panel. The symbols represent different plasma densities, from above $n_e = 10^{15}$ m^{-3} (×), $n_e = 5 \times 10^{14}$ m^{-3} (+), $n_e = 10^{14}$ m^{-3} (◊), $n_e = 5 \times 10^{13}$ m^{-3} (□), and $n_e = 10^{13}$ m^{-3} (○).

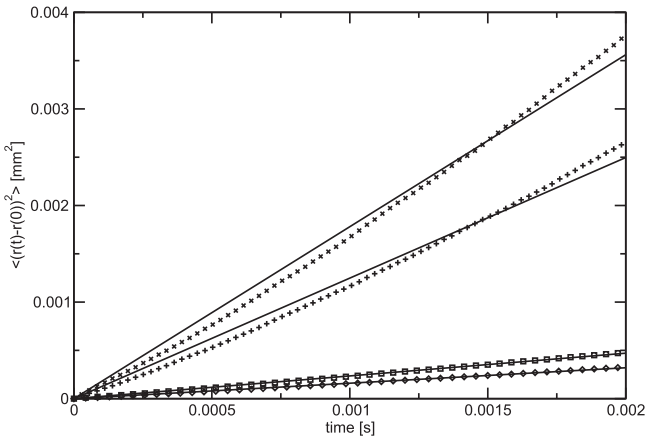

Figure 4. Time evolution of the average radial position of the antiproton, excluding the effects of antihydrogen formation. Here $n_e = 10^{15}$ m^{-3}, and $T_e = 30$ K, $B = 1$ T (×), $T_e = 15$ K, $B = 1$ T (+), $T_e = 30$ K, $B = 3$ T (□), and $T_e = 15$ K, $B = 3$ T (◊). The lines are fits to $\langle (r(t) - r(0))^2 \rangle \propto t$, as is characteristic for thermal Brownian motion.

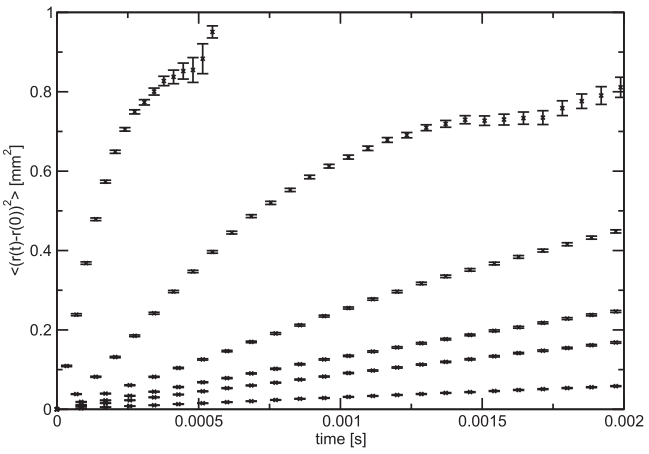

Figure 5. Change in average radial position, $\langle (r(t) - r(0))^2 \rangle$ of the antiprotons as a function of time and for different temperatures. The data are for 10, 15, 20, 25, 30 and 50 K with the upper curve being that for the lowest temperature, and with the remainder in order of increasing T_e. In all cases $n_e = 10^{15}$ m^{-3} and $B = 3$ T. The error bars show the standard error of the mean.

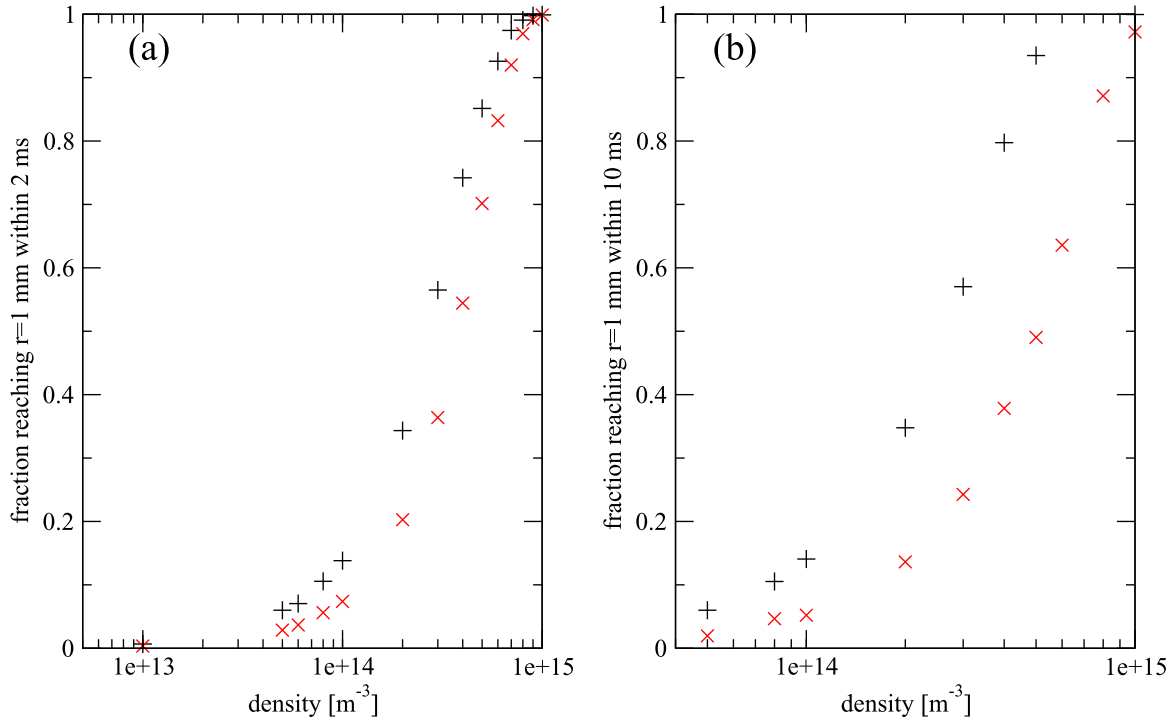

Figure 6. (a) Fraction of antiprotons reaching $r = 1$ mm, within 2 ms as a function of density for a $T_e = 15$ K plasma and $B = 1$ T (black, +) and 3 T (red, ×), (b) same but $T_e = 30$ K and waiting time 10 ms.

This naive estimate contains no plasma effects. Comparing to the full treatment in [42] we find, within the relevant parameter range, an approximate agreement if $\Delta r_{\bar{p}}$ is multiplied by the dimensionless parameter $\xi = \lambda_D k_{max}$, where $\lambda_D = \sqrt{k_B T_e \epsilon_0/(e^2 n_e)}$ is the Debye length of the plasma, and k_{max} is a high momentum/short distance cut off. (Note that ξ varies from 1–3 over the full parameter range explored in this work.) Here we take $k_{max} = n_e^{1/3}$. Thus we find

$$\lambda_{ep}\Delta r_{\bar{p}}^2 = C\frac{8n_e}{\pi T_e^{1/2}}\frac{k_B m \xi^2}{(eB)^2} = C'\frac{n_e^{2/3}T_e^{1/2}}{B^2}, \tag{13}$$

where

$$C' = C\frac{8k_B^2 m\epsilon_0}{\pi e^4} = \sqrt{\frac{mk_B}{2}}\left(\frac{1}{\pi^{7/2}\epsilon_0}\right). \tag{14}$$

Inserting values for the constants it is found that $C' = 5.2 \times 10^{-18}$ m^4 s^{-1} T^2 K$^{-1/2}$, which for $B = 3$ T, $n_e = 10^{15}$ m^{-3} and $T_e = 15$ K yields $\lambda_{ep}\Delta r_{\bar{p}}^2 \simeq 2.2 \times 10^{-8}$ m^2 s^{-1}, which is roughly comparable to the result from the simulation (see figure 4). Further, the scalings with T_e and B also roughly agree with the results in figure 4.

The next step is to estimate the size of the jumps made as antihydrogen, which is taken to be the thermal $\overline{\mathrm{H}}$ speed (which is assumed to be that of the antiproton), multiplied by its time of flight before destruction in collision. Thus we can write

$$\Delta r_{\overline{\mathrm{H}}} = v_{\overline{\mathrm{H}}}/n_e\sigma_{\overline{\mathrm{H}}}v_e = \sqrt{\frac{m}{M}}\frac{1}{n_e\sigma_{\overline{\mathrm{H}}}}, \tag{15}$$

with $n_e\sigma_{\overline{\mathrm{H}}}v_e$ the break-up collision frequency, where $\sigma_{\overline{\mathrm{H}}}$ is some average break-up cross section for the highly excited states of antihydrogen that exist fleetingly in the plasma. Putting numbers ($n_e = 10^{15}$ m^{-3} and $\sigma_{\overline{\mathrm{H}}} = 10^{-12}$ m^2) into (15) we find $\Delta r_{\overline{\mathrm{H}}} \approx 2.3 \times 10^{-5}$ m. This is comparable to the average of $|\Delta r_{\overline{\mathrm{H}}}|$ in figure 1 (when, as discussed above, only $\Delta r_{\overline{\mathrm{H}}} < 1$ mm are included in the average). This shows that our estimate for $\sigma_{\overline{\mathrm{H}}}$ is reasonable. However, the thermal velocity will be isotropic, and thus give rise to a $\Delta r_{\overline{\mathrm{H}}}$ which is symmetric around zero, i.e. $\langle\Delta r_{\overline{\mathrm{H}}}\rangle = 0$. This gives only a contribution to diffusion, which we neglect compared to the diffusion of the $\bar{p}$s in their bare state, that is, we ignore the fluctuations in the $\overline{\mathrm{H}}$ transport, and hence approximate $\langle\Delta r_{\overline{\mathrm{H}}}^2\rangle = \langle\Delta r_{\overline{\mathrm{H}}}\rangle^2$.

The net outward drift is instead given by the rotational $\mathbf{E} \times \mathbf{B}$ drift velocity of the $\bar{p}$ (introduced in section 1), which upon formation is transferred to the $\overline{\mathrm{H}}$ as a tangential velocity $\mathbf{v}_T = en_e r_0/(2\epsilon_0 B)\hat{\mathbf{y}} = v_T\hat{\mathbf{y}}$, where we take $\hat{\mathbf{y}}$ to be the direction tangential to the $\bar{p}$ motion at the time $t = t_0$ of formation (here $r_0 = r(t_0)$). This means that $\mathbf{r}(t_0) = r_0\hat{\mathbf{x}}$. The total velocity is then $\mathbf{v}_{\overline{\mathrm{H}}} = v_{th}^x\hat{\mathbf{x}} + (v_{th}^y + v_T)\hat{\mathbf{y}}$, where v_{th}^i is the thermal velocity in the i-direction, which averages to zero. As such, the change in radial position is given by $\Delta r_{\overline{\mathrm{H}}} = \sqrt{(r_0 + v_{th}^x\Delta t)^2 + (v_{th}^y + v_T)^2\Delta t^2} - r_0$, where Δt is the time between formation and ionisation. For short jumps $\Delta r_{\overline{\mathrm{H}}} \ll r_0$ one has $\Delta r_{\overline{\mathrm{H}}} \simeq v_{th}^x\Delta t + (v_{th}^y + v_T)^2\Delta t^2/(2r_0)$, and hence $\langle\Delta r_{\overline{\mathrm{H}}}\rangle \simeq ((v_{th}^y)^2 + v_T^2)\Delta t^2/(2r_0)$. In the opposite limit $\Delta r_{\overline{\mathrm{H}}} \simeq \sqrt{(v_{th}^x)^2 + (v_{th}^y + v_T)^2}\,\Delta t$, that is linear in Δt, and $\langle\Delta r_{\overline{\mathrm{H}}}\rangle \simeq v_T\Delta t$. Since $v_T \propto n_e$ the product $v_T\Delta t$ is independent of positron density, and we expect $\rho(\Delta r_{\overline{\mathrm{H}}})$ to be largely independent of density for large $\rho(\Delta r_{\overline{\mathrm{H}}})$. For relevant parameters ($B = 3$ T, $n_e = 10^{15}$ m^{-3} and $T = 15$ K) we find that the long jumps should give the dominating

contribution to the $\overline{\mathrm{H}}$ transport, a result which is confirmed by simulations.

We now write the formation rate for the three-body reaction in terms of n_e and T_e as $\lambda_{\overline{\mathrm{H}}} = C'' n_e^2 T_e^{-k}$, where for the moment the T_e dependence is parameterised in terms of the exponent, k, noting that $k = 4.5$ applies in equilibrium for the production of antihydrogen bound deeply enough to survive further collision. From this it is easy to show, after a little substitution, that

$$\lambda_{\overline{\mathrm{H}}} \langle \Delta r_{\overline{\mathrm{H}}} \rangle = \frac{C'' e \langle r_0 \rangle}{2\epsilon_0 B \sigma_{\overline{\mathrm{H}}}} \sqrt{\frac{\pi m}{2k_B}} n_e^2 T_e^{-(k+1/2)}. \tag{16}$$

This is likely to drop rapidly with T_e. (Here it is assumed that the break-up cross section is independent of the plasma parameters, but this may not be true, due to the nature of the weakly bound states.)

We now perform a crude estimate of $\lambda_{\overline{\mathrm{H}}} \langle \Delta r_{\overline{\mathrm{H}}} \rangle$. It would be possible to use the zero-field equilibrium three-body coefficient for $C'' = 4 \times 10^{-21}\,\mathrm{m^6\,s^{-1}\,K^{9/2}}$: as a result the value $k = 4.5$ would apply. However, as noted above, this is the rate applicable for the formation of antihydrogen that is bound deeply enough to survive further collisions, which is not the case here. It is, however, possible to use the data generated from the simulations at $n_e = 10^{15}\,\mathrm{m^{-3}}$ to find values for C'' and k for the 'in plasma' case (see table 2). These turn out to be $C'' = 10^{-20}\,\mathrm{m^6\,s^{-1}\,K^{4.3}}$ and $k = 4.3$. Thus at $n_e = 10^{15}\,\mathrm{m^{-3}}$ and $T_e = 15\,\mathrm{K}$, $B = 3\,\mathrm{T}$, $\langle r_0 \rangle = 0.1$ mm and assuming $\sigma_{\overline{\mathrm{H}}} = 10^{-12}\ \mathrm{m^{-2}}$ (there is evidence that the initial states are of micron size [33, 44], hence this estimate) it is found that $\lambda_{\overline{\mathrm{H}}} \langle \Delta r_{\overline{\mathrm{H}}} \rangle \approx 2.2\ \mathrm{m\,s^{-1}}$, which is of the same order of magnitude as observed in simulations.

We can now also estimate the fraction of time the $\bar{p}$ is bound inside a $\overline{\mathrm{H}}$. From (4)

$$F_{\overline{\mathrm{H}}} = \frac{\lambda_{\overline{\mathrm{H}}} \langle \Delta t \rangle}{1 + \lambda_{\overline{\mathrm{H}}} \langle \Delta t \rangle} \simeq \frac{C'' n_e^2 T_e^{-k}}{n_e \sigma_{\overline{\mathrm{H}}} v_e + C'' n_e^2 T_e^{-k}}. \tag{17}$$

For the parameters used above $F_{\overline{\mathrm{H}}} \simeq 0.004$, and we shall therefore approximate $1 - F_{\overline{\mathrm{H}}} \simeq 1$. This is consistent with [21], where it was stated that the antiprotons only spend about 1% of their time as antihydrogen. Furthermore, from (9), (13), (14) and (16) R can be represented as

$$R = \frac{\pi^4 C'' e}{2k_B \sigma_{\overline{\mathrm{H}}}} r \langle r_0 \rangle B n_e^{4/3} T_e^{-5.3} = C''' B n_e^{4/3} T_e^{-5.3}. \tag{18}$$

Inserting numbers for C'' and using the above value for $\sigma_{\overline{\mathrm{H}}} = 10^{-12}\ \mathrm{m^{-2}}$, $r = 1$ mm as in our simulations, and $\langle r_0 \rangle \sim 0.1$ mm we find that $C''' \approx 5.6 \times 10^{-10}\,\mathrm{T^{-1}\,m^4\,K^{-5.3}}$. Using $B = 3\,\mathrm{T}$, $n_e = 10^{15}\ \mathrm{m^{-3}}$ and $T = 15\,\mathrm{K}$, we find that $R \sim 9.7 \times 10^4$, i.e. the radial transport is totally dominated by antihydrogen formation. It is interesting to note that at very early times (small r) thermal diffusion will dominate; that is, if the $\bar{p}$ originate on the trap axis there will initially be no transport due to the antihydrogen formation process, because $v_T = 0$. For the parameters above thermal transport dominates while $r \lesssim 5\,\mu\mathrm{m}$. In a real experiment, unless antiproton injection is restricted to such a narrow radius, transport due to antihydrogen formation will dominate at all times.

Varying the parameters, the roles may be reversed. For instance still at $B = 3\,\mathrm{T}$ and $n_e = 10^{15}\ \mathrm{m^{-3}}$ thermal transport will dominate for $T_e \gtrsim 130\,\mathrm{K}$. Reducing the density to $n_e = 10^{13}\ \mathrm{m^{-3}}$ and the magnetic field to $B = 1\,\mathrm{T}$, thermal diffusion dominates for $T_e \gtrsim 35\,\mathrm{K}$. According to our simulations, at this density thermal diffusion dominates already at $T_e = 15\,\mathrm{K}$. However, given the crudeness of our estimate, we conclude that it is in fair agreement with our numerical results. In particular, we expect the very sharp dependence on temperature to be correct.

4. Concluding remarks

We have identified a mechanism for radial antiproton transport in magnetised positron plasmas: namely the repeated formation and ionisation of antihydrogen atoms. We show through simulations that this is the dominant radial transport process within most of the parameter range relevant for current experiments. We also provide a simple model for the relative rate of antiproton transport both through antihydrogen formation, and through thermal diffusion. This model predicts a sharp dependence on temperature of the relative rates, which is consistent with the results from our simulations.

The most recent experiments, where positron densities close to the lower end of the parameter range used in our simulations are typically used [3–12], may be operating in a region where the thermal and $\overline{\mathrm{H}}$ formation mechanisms are comparable in magnitude. If this is the case, then as T_e is further reduced, which is a major goal of the current experiments, radial antiproton transport is likely to increase sharply. Further work will include investigating the latter at higher densities, such as those suggested in [45], where we expect qualitatively new features arising from the mismatch between the drift velocities of the antiprotons and the positrons.

Acknowledgments

This research was supported by the EPSRC (UK) and the Swedish Research Council (VR).

References

[1] Amoretti M *et al* (ATHENA Collaboration) 2002 *Nature* **419** 456
[2] Gabrielse G *et al* (ATRAP Collaboration) 2002 *Phys. Rev. Lett.* **89** 213401
[3] Andresen G B *et al* (ALPHA Collaboration) 2010 *Nature* **468** 673
[4] Andresen G B *et al* (ALPHA Collaboration) 2011 *Nat. Phys.* **7** 558
[5] Andresen G B *et al* (ALPHA Collaboration) 2011 *Phys. Lett.* B **695** 95
[6] Gabrielse G *et al* (ATRAP Collaboration) 2012 *Phys. Rev. Lett.* **108** 113002
[7] Enomoto Y *et al* 2010 *Phys. Rev. Lett.* **105** 243401
[8] Kuroda N *et al* 2014 *Nat. Commun.* **5** 3089
[9] Amole C *et al* (ALPHA Collaboration) 2012 *Nature* **483** 439

[10] Amole C *et al* (ALPHA Collaboration) 2013 *Nat. Commun.* **4** 1875
[11] Amole C *et al* (ALPHA Collaboration) 2014 *Nat. Commun.* **5** 3955
[12] Ahmadi M *et al* (ALPHA Collaboration) 2016 *Nature* **529** 373
[13] Maury S 1997 *Hyperfine Interact.* **109** 43
[14] Eriksson T 2009 *Hyperfine Interact.* **194** 123
[15] Major F H, Gheorge V N and Werth G 2005 *Charged Particle Traps: Physics and Techniques of Charged Particle Field Confinement* (Berlin: Springer)
[16] Ghosh P K 1995 *Ion Traps* (Oxford: Clarendon)
[17] Brown L S and Gabrielse G 1988 *Rev. Mod. Phys.* **58** 233
[18] Gabrielse G, Rolston S L, Haarsma L and Kells W 1988 *Phys. Lett.* A **129** 38
[19] Holzscheiter M H, Charlton M and Nieto M M 2004 *Phys. Rep.* **402** 1
[20] Robicheaux F 2008 *J. Phys. B: At. Mol. Opt. Phys.* **41** 192001
[21] Jonsell S, van der Werf D P, Charlton M and Robicheaux F 2009 *J. Phys. B: At. Mol. Opt. Phys.* **42** 215002
[22] Amoretti M *et al* (ATHENA Collaboration) 2004 *Phys. Lett.* B **590** 133
[23] Andresen G B *et al* (ALPHA Collaboration) 2010 *Phys. Lett.* B **685** 141
[24] Gabrielse G *et al* (ATRAP Collaboration) 2002 *Phys. Rev. Lett.* **89** 233401
[25] Mansbach P and Keck J 1969 *Phys. Rev.* **181** 275
[26] Müller A and Wolf A 1997 *Hyperfine. Interact.* **109** 233
[27] Gabrielse G *et al* (ATRAP Collaboration) 2004 *Phys. Rev. Lett.* **93** 073401
[28] Amoretti M *et al* (ATHENA Collaboration) 2004 *Phys. Lett.* B **578** 23
[29] Amoretti M *et al* (ATHENA Collaboration) 2004 *Phys. Lett.* B **583** 59
[30] Madsen N *et al* (ATHENA Collaboration) 2005 *Phys. Rev. Lett.* **94** 033403
[31] Robicheaux F and Hanson J D 2004 *Phys. Rev.* A **69** 010701
[32] Robicheaux F 2004 *Phys. Rev.* A **70** 022510
[33] Pohl T, Sadeghpour H R and Gabrielse G 2006 *Phys. Rev. Lett.* **97** 143401
[34] Correa C E, Correa J R and Ordonez C A 2005 *Phys. Rev.* E **72** 046046
[35] Hu S X, Vrinceanu D, Mazevet S and Collins L A 2005 *Phys. Rev. Lett.* **95** 163402
[36] Kuzmin S G and O'Neil T M 2004 *Phys. Rev. Lett.* **92** 23401
[37] Kuzmin S G and O'Neil T M 2005 *Phys. Plasmas* **12** 012101
[38] Vrinceanu D, Hu S X, Mazevet S and Collins L A 2005 *Phys. Rev.* A **72** 042503
[39] Robicheaux F 2006 *Phys. Rev.* A **73** 033401
[40] Topçu T and Robicheaux F 2006 *Phys. Rev.* A **73** 043405
[41] Vrinceanu D, Granger B E, Parrott R, Sadeghpour H R, Cederbaum L, Mody A, Tan J and Gabrielse G 2004 *Phys. Rev. Lett.* **92** 133402
[42] Nersisyan H B, Walter M and Zwicknagel G 2000 *Phys. Rev.* E **61** 7022
[43] Vlahos L, Isliker H, Kominis H and Hizanidis K 2008 (arXiv:0805.0419)
[44] Gabrielse G 2005 *Adv. At. Mol. Opt. Phys.* **50** 155
[45] Radics B, Murtagh D J, Yamazaki Y and Robicheaux F 2014 *Phys. Rev.* A **90** 032704